# Application of Laser Welding in Car Bodies Manufacturing

**J Viňáš[1], J Brezinová[1], J Brezina1, P Maruschak[2] and S Panin[3]**

[1]Technical University of Košice, Mäsiarska 74, 040 01 Košice, Slovakia
[2]Ternopil National Ivan Pul'uj Technical University, Rus'ka str. 56, 46001 Ternopil, Ukraine
[3]Institute of Strength Physics and Materials Science of Siberian Branch of Russian Academy of Sciences, 634055 Tomsk, Russia

svp@ispms.ru

**Abstract**. The paper deals with a problem of laser welding of zinc-coated steel (DX53D+Z and DX54D+Z) plates. Experiments were carried out with the use of steel plates 0.8; 1.0; 1.3; and 1.75 mm thick. High power 2.5-2.9 kW $CO_2$ laser was employed. $CO_2$ was used as the shielded gas. The optimal parameters of welding for material under study were determined. The mechanical properties of welded joints were measured through the tensile loading and microhardness measurement. Tensile performances of the specimens fabricated at different welding rate and laser beam power were compared with that of the base material.

## 1. Introduction

Combined tailored welded blanks (TWB) consist of two or more joined pieces and they can represent a combination of materials of different thickness and grades. These tailored welded blanks found their application mostly in automobile industry where reliably is of crucial importance. The joining technique allows one to influence hardness, stiffness or corrosive resistance of metal sheets in different parts of the component. In doing so, the hardness might be increased, while parts of different thickness might be connected even being covered with protective layers (foils) [1-4].

It is known that zinc melts at a temperature of 906 ° C, while steel at 1100 ° C. With the conventional method of welding, the coating is damaged inevitably. During laser welding of galvanized steel sheets, a high-pressure evaporation region (66–1060 atm) arises around the melt with a temperature of 1600–3000 °C [5-7]. If the gap between the sheets is narrow, the vapor cannot go away, deviations occur in the pressure of the vapor-gas channel, and damage takes place. An explosive degassing process disrupts the welding process, and the vapor-gas channel is destroyed due to pressure imbalance. A large volume of molten steel is forced out of the molten pool, which leads to the formation of shells, imperfections or pores in the weld metal, which affect the mechanical properties of the weld [8–10]. The output and the laser welding rate were taken as fundamental parameters affecting the quality of the welds. Note, that the output is the most critical factor in the laser welding operation [11-15].

The aim of the study is to evaluate the application of laser welding technology for joining the materials of specified thickness. Improper external and internal welding parameters were found using non–destructive and destructive (mechanical) tests. Also, some reasons for the structure heterogeneity nucleation in the welds and their influence on mechanical properties were revealed. In doing so,

standard and small test coupons were examined at two loading rates. The next parts of the paper deals with the study of Zn surface layer behaviour of the combined tailored blanks during the welding process. To this end, the microhardness of welds was measured. The possibility of the formation of martensite phase is shown and discussed.

## 2. Experimental part

The material under study was thermally zinc-coated with steel sheets (10.0 – 12.5 μm thick) used in the automobile industry [1]. Samples were welded by $CO_2$ laser ELB5. The following welding parameters were used: TWB1 = 2.5 kW, TWB2 = 2.9 kW; welding rate was 45 mm /s$^{-1}$, the pressure of protective gas Ar was 0.2 MPa, beam was focused at the surface. Welds were non–destructively tested by visual examination (according to EN ISO 17637:2016), as well as Penetrant inspection (PT) according to EN ISO 23277:2010 for the detection of surface faults. Radiographic testing was employed to detect internal faults (EN 12517-1:2006-10). Chemical composition and mechanical properties (yield strength - $\sigma_{ys}$; tensile strength – $\sigma_{ts}$; elongation at break – $\varepsilon_t$ [%]) of tested materials i) DX53D+Z and ii) DX54D+Z EN 10346: 2015 are shown in Table 1 and Table 2.

**Table 1.** TWB1 – materials combination.

|  | Thickness | Chemical composition of TWB 1 (wt. %), Fe - bal. | | | | | | | |
|---|---|---|---|---|---|---|---|---|---|
| Material | (mm) | $C_{max}$ | $Mn_{max}$ | $P_{max}$ | $S_{max}$ | $Si_{max}$ | Al | Ti | $N_{max}$ |
| DX53D+Z | 1 | 0.04 | 0.20 | 0.015 | 0.012 | 0.01 | 0.03-0.06 | | 0.006 |
| DX54D+Z | 0.8 | 0.015 | 0.20 | 0.015 | 0.015 | | min 0.02 | 0.06-0.14 | 0.006 |
| Mechanical properties$^{1)}$ | | | | | | | | | |
| Material | $\sigma_{ys}$ (MPa) | | $\sigma_{ts}$ (MPa) | | $\varepsilon_t$ (%) | | Bending angle 180° | | |
| DX53D+Z | 260 | | max. 380 | | 30 | | 0.a | | |
| DX54D+Z | 220 | | max. 350 | | 36 | | 0.a | | |

**Table 2.** TWB2 – materials combination.

|  | Thickness | Chemical composition of TWB2 (wt. %), Fe - bal. | | | | | | | | |
|---|---|---|---|---|---|---|---|---|---|---|
| Material | (mm) | $C_{max}$ | $Mn_{max}$ | $P_{max}$ | $S_{max}$ | $Si_{max}$ | Al | Ti | $Nb_{max}$ | $N_{max}$ |
| DX53D+Z | 1.75 | 0.04 | 0.20 | 0.015 | 0.012 | 0.01 | 0.03-0.06 | | | 0.006 |
| DX54D+Z | 1.3 | 0.01 | 0.6 | 0.025 | 0.08 | 0.04 | 0.15 | 0.04 | 0.003 | |
| Mechanical properties $^{1)}$ | | | | | | | | | | |
| Material | $\sigma_{ys}$ (MPa) | | $\sigma_{ts}$ (MPa) | | $\varepsilon_t$ (%) | | Bending angle 180° | | | |
| DX53D+Z | 260 | | max. 380 | | 30 | | 0.a | | | |
| DX54D+Z | 260 | | max. 350 | | 24 | | 0.a | | | |

$^{1)}$Tests were done in the transversal direction in regard to rolling direction

Then, mechanical testing of the specimens was carried out. Tensile test (according to EN ISO 4136:2011-09) were performed for the samples with a transverse welds of standard and reduced dimension. Also, the different loading rate was employed. For the standard (S) (*l* = 80 mm) (figure 1) and non – standard (*N*) (*l* = 30 mm) (figure 2) samples, the loading rate was *v*=30 mm . min$^{-1}$ and *v*=0.9 mm . min$^{-1}$ respectively. Metallographic analysis and microhardness measurement were conducted according to EN ISO 9015-2:2011-09 (HV0.01).

The EDX analysis over the specimens' cross section was conducted with further microhardness measurement in the WM (weld metal) and heat affected zone (HAZ).
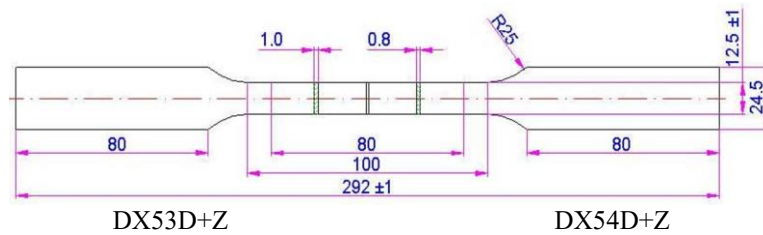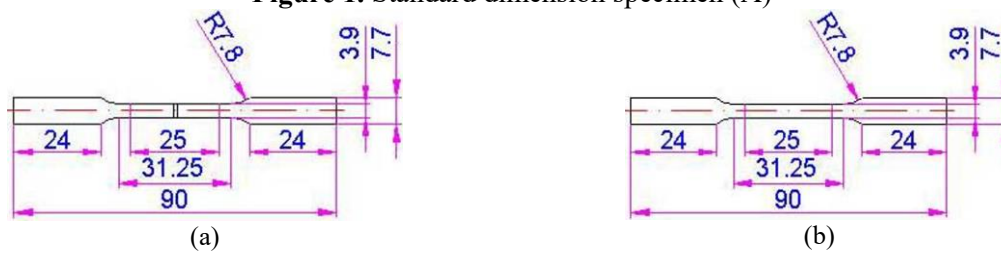
**Figure 1.** Standard dimension specimen (A)



**Figure 2.** Non – standard (low dimension) test specimen with (a) and without weld (b).

## 3. Results and discussed

### 3.1. *Tensile test*

Data on mechanical properties measured under tensile tests for the TWB1 and TWB2 are shown in Table 3 and Table 4. It is seen that presence of defects does not affect mechanical response substantially (see their description below). The non–standard samples („N") did not fail over the weld region. High thermal output, as well as high cooling rate, stimulates the formation of fine microstructure within the narrow width weld.

Further inspection of the weld does not reveal high porosity level. In so doing, the pores do not exert any reducing impact onto the tensile properties of the welded joint. However, it can be caused by the high hardness of the WM and HAZ regions, which effectively protects faulty (defective) weld from fast fracture.

**Table 3.** Average values of mechanical properties (Base metal/TWB1).

| Mechanical properties | Base metal DX54D+Z – 0.8 mm | | | Welded joint - TWB1 | | | | | |
|---|---|---|---|---|---|---|---|---|---|
| | $v = 30$ mm.min$^{-1}$A | $v = 0.9$ mm.min$^{-1}$B | $v = 30$ mm.min$^{-1}$B | $v = 30$ mm.min$^{-1}$A | | | $v = 0.9$ mm.min$^{-1}$B | | $v = 30$ mm.min$^{-1}$B |
| $\sigma_{ys}$ [MPa] | 192 $^{S}$ | 173 | 200 | 187 $^{S}$ | 183* | -184 | 189* | 192 | 217 |
| $\sigma_{ts}$ [MPa] | 291 $^{S}$ | 275 | 295 | 298 $^{S}$ | 291* | -297 | 287* | 289 | 304 |
| $\varepsilon_{t}$ [%] | 37.7 $^{S}$ | 31.9 | 30.9 | 27.2 $^{S}$ | 21.2* | 27.2 | 21.2* | 26.2 | 22.3 |

**Table 4.** Average values of mechanical properties (Base metal/TWB2).

| Mechanical properties | Base metal DX53D+Z - 1.3 mm | | | Welded join – TWB2 | | | | |
|---|---|---|---|---|---|---|---|---|
| | $v = 30$ mm.min$^{-1}$A | $v = 0.9$ mm.min$^{-1}$B | $v = 30$ mm.min$^{-1}$B | $v = 30$ mm.min$^{-1}$A | | $v = 0.9$ mm.min$^{-1}$B | | $v = 30$ mm.min$^{-1}$B |
| $\sigma_{ys}$ [MPa] | 312 $^{S}$ | 311 | 338 | 321 $^{S}$ | -319 | 336.67 | | 347 |
| $\sigma_{ts}$ [MPa] | 389.6 $^{S}$ | 376.7 | 400 | 396 $^{S}$ | -392 | 385 | | 396 |
| $\varepsilon_{t}$ [%] | 24.9 $^{S}$ | 20.3 | 24.2 | 19.1 $^{S}$ | -19.03 | 15.33 | | 17.9 |

S – standard dimension test specimens (A); (-) – standard dimension test specimens with damaged welds

Radiometric inspection possesses high sensitivity to reveal faults in weld metal. However, the tensile tests performed on the non-standard and standard size sample showed low sensitivity to presence of faults. In so doing, high strength of the weld supresses development of faults. The variation of key mechanical properties was evaluated through measurement of Tensile strength/Yield strength and elongation at break. The results obtained evidence that with increasing loading rate, a slight increase in the Tensile strength/Yield strength and elongation at break takes place.

### 3.2. *Microhardness and metalograph*

Average values of microhardness measured for the TWB1 tensile test specimens no. 3 and no. 4 are shown in Table 5. Average values of microhardness measured for the TWB2 tensile test specimens no. 1 and no. 2 are shown in Table 6. The data of their optical microscopy observation is illustrated by figure 3 and figure 4. Microstructure of the base metal DX54D+Z represents ferrite pattern and grains of the polyedrical shape. The DX53D+Z has ferrite-cementite structure; however, cementite is hardly seen over the sample cross section. The laser weld metal has a characteristic dendrite structure.

**Table 5.** Average values of microhardness of TWB1.

| No. | Location of measurement | Specimen no.3 | Specimen no.4 |
|-----|------------------------|---------------|---------------|
| 1 | Base metal 1 DX53D+Z (1 mm) | 106 | 110 |
| 2 | HAZ1 DX53D+Z (1 mm) | 122 | 125 |
| 3 | WELD | 229 | 256 |
| 4 | HAZ 2 DX54D+Z (0.8 mm) | 111 | 118 |
| 5 | Base metal 2   DX54D+Z (0.8 mm) | 102 | 104 |

**Table 6.** Average values of microhardness of TWB2.

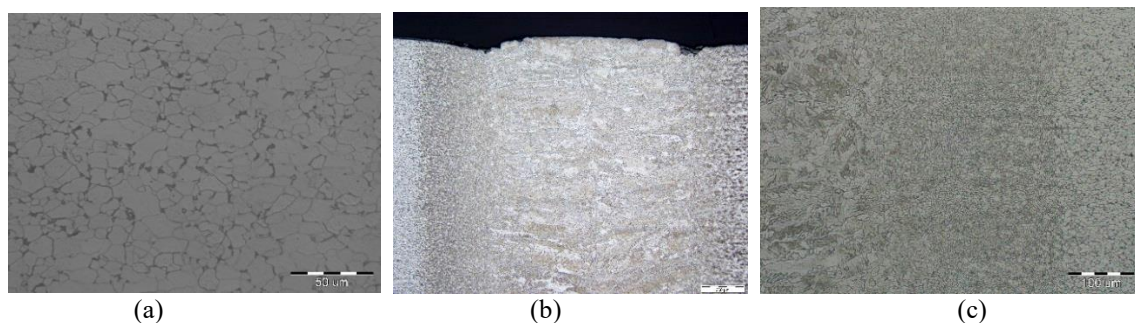| No. | Location of measurement | Specimen no.1 | Specimen no.2 |
|-----|------------------------|---------------|---------------|
| 1 | Base metal 1 DX53D+Z (1.75 mm) | 112 | 108 |
| 2 | HAZ1 DX53D+Z (1.75 mm) | 126 | 129 |
| 3 | WELD | 235 | 242 |
| 4 | HAZ 2 DX54D+Z (1.3 mm) | 125 | 124 |
| 5 | Base metal 2  DX54D+Z (1.3 mm) | 108 | 113 |

|  |  |  |
|---|---|---|
| (a) | (b) | (c) |

**Figure 3.** Structure of welded joint TWB1: a - base metal DX53D+Z; b – weld; c – HAZ 2 DX54D+Z.

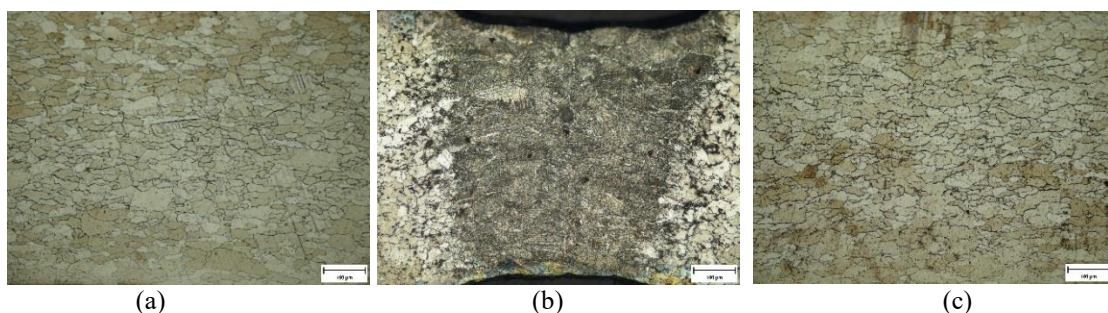|  |  |  |
|---|---|---|
| (a) | (b) | (c) |

**Figure 4.** Structure of welded joint TWB2: a - base material DX53D+Z; b - weld and HAZ;
c - base material DX54D+Z.

The structure of the weld has a gradient pattern. It consists of a fusion zone; an overheated zone is located on the boundary of the zone of molten metal, which was not subjected to melting, and a normalization zone with a fine-grained structure. The fusion zone is formed by round-shaped grains, figure 4a, oriented at an angle to the center of the weld. In general, microalloyed steels are less

incoherent over the austenite phase growth in the HAZ because of its blocking by the precipitates. Most dangerous effect of structure modification consists in increasing the size of the overheating zone, especially in the upper part of the weld, since the welded metal has the lowest strength properties there. The thin sheets, i.e. TWB1, tends to be more sensitive to the welding parameters.

Part of the study was dedicated to monitoring the uprising defects, i.e. pores in the weld. Figure 5 shows the pore in the region where the EDX analysis was conducted. However, diffusion of Zn from the protective layer into the weld metal is not revealed. An increased content of oxygen and aluminium was detected at the pores [1]. In the TBW1 sample, some particles become evident in the weld. The reason is related to the edge treatment procedure (grooving). Note that edges were not properly treated before the welding [16]. Welding of the thin sheets (TWB1) exhibits high sensitivity to the width of the weld. In doing so, air coming from the voids was the main reason for the nucleation of plenty of pores.
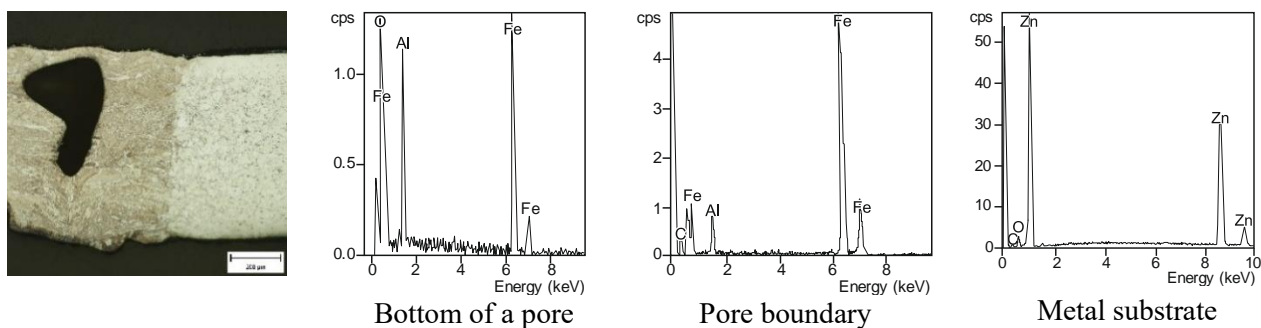


**Figure 5.** Micrograph of a pore and data of the EDX analyses.

When ensuring higher welding quality for the TWB2, the nucleation of pores was revealed. However the level of defectiveness was admissible (ranking to 1 – 3 points). At the same time, the 80% of TWB1 welds contains too many defects and their level of defectiveness is estimated as non-acceptable.

With the use of penetrant inspection, pores were revealed on the surface of welds. For steels (DX53D+Z and DX54D+Z), they mainly comes from aluminum oxides and nitrides [17]. Gas porosity and gas bubbles can also arise due to a release of gases dissolved in the metal during welding process.

A decrease in the welding speed while maintaining other parameters of the process eliminates shrinkage cavities primarily in the upper part of the weld. However, it gives rise to nucleation of an equally dangerous defect - the formation of a penetration zone with an unstable width of the weld. At the same time, an active formation of defects in the heat affected zone is normally accompanied by the redistribution of chemical elements and even dispersed phases, which in turn stimulates the processes of phase formations in the metal [18, 19]. Moreover, phase formations of certain sizes can "strengthen" grain boundaries, contributing to the refinement of the structure.

Laser welding is one of the promising methods of car bodies manufacturing. But since the nucleation of defects such as pores, holes, lack of penetration cannot be excluded completely, the post-processing inspection of products should be obligatory applied.

## 4. Conclusion

The key factors of the technological parameters of laser welding of zinc-coated steel sheets (DX53D + Z and DX54D + Z) plates affecting structure formation as well as strength of the weld have been determined. It is found that the weld structure has a gradient pattern. Technological recommendations are formulated to reduce the defectiveness of the structure in the primary crystallization zone as well as the overheating zone, based on the morphology analysis of the resulting pores and weld as a whole.

**Acknowledgement**

**References**

*[1]*      Viňáš J 2000 Laser technologies used in welding of surface treated materials *Diploma thesis, Košice*
[2]      Razmpoosh M H, et al. 2018 *Materials & Design* **155** pp 375-383
[3]      Deng S et al. 2019 *Int. J. of Heat and Mass Transfer* **140** pp 269-280
[4]      Sejč P and Világoš T Strojnicky Casopis 2018 68 pp 89-94
[5]      Gaoyang M, Lingda X, Chunming W, Ping J and Guoli Z 2019 *Materials & Design* **181** Art. number 107980
[6]      Čičo P, Kalincová D and Kotus M 2011 *Research in Agricult. Eng.* **57** pp 50-55
[7]      Wahba M, Kawahito Y and Katayama S 2011 *30-th Int. Cong. on Applications of Lasers and Electro-Optics* ICALEO pp 343-349
[8]      Zdravecká E and Slota J 2019 *Metals* **9** (91) https://doi.org/10.3390/met9010091
[9]      Kim J, Oh S, Son M and Ki H 2017 *J. of Mat. Proc. Tech.* **249** pp 135-148
[10]     Hong K-M, Shin YC, 2017 *J. of Mat. Proc. Tech.* **245** pp 46-69
[11]     Kim J, Oh S and Ki H 2016 *J. of Mat. Proc. Tech.* **232** pp 131-141
[12]     Fengde L et al. 2019 *Mat. Research Express* **6** Art. number 076505
[13]     Vyskoč M, Sahul M and Sahul M 2018 *J. of Mat. Eng. and Performance* **27** pp 2993-3006
[14]     Sahul M, Turna M and Sahul M 2014 *Magnesium Technology 2014 - TMS 2014 143rd Annual Meeting and Exhibition* San Diego CA United States pp 301-305
[15]     Viňáš J and Ábel M 2015 *Materials Science Forum, International Conference on Surface Engineering and Materials in Mechanical Engineering* High Tatras Slovakia **818** pp 239-242
[16]     Vuherer T, Maruschak P O and Samardžić I 2012 *Metalurgija* **51** pp 301-304
[17]     Viňáš J, Brezinová J, Brezina J and Maruschak P O 2019 *Materials Science* **55** 1 pp 46-51
[18]     Konovalov S, Kormyshev V, Gromov V and Ivanov Yu 2016 *Mater. Sci. Forum* **870** pp 159-162